

DC and RF Characteristics of 0.15 μm Power Metamorphic HEMTs

Jae Yeob Shim, Hyung-Sup Yoon, Dong Min Kang, Ju Yeon Hong, and Kyung Ho Lee

DC and RF characteristics of 0.15 μm GaAs power metamorphic high electron mobility transistors (MHEMT) have been investigated. The 0.15 $\mu\text{m} \times 100 \mu\text{m}$ MHEMT device shows a drain saturation current of 480 mA/mm, an extrinsic transconductance of 830 mS/mm, and a threshold voltage of -0.65 V. Uniformities of the threshold voltage and the maximum extrinsic transconductance across a 4-inch wafer were 8.3% and 5.1%, respectively. The obtained cut-off frequency and maximum frequency of oscillation are 141 GHz and 243 GHz, respectively. The 8 \times 50 μm MHEMT device shows 33.2% power-added efficiency, an 18.1 dB power gain, and a 28.2 mW output power. A very low minimum noise figure of 0.79 dB and an associated gain of 10.56 dB at 26 GHz are obtained for the power MHEMT with an indium content of 53% in the InGaAs channel. This excellent noise characteristic is attributed to the drastic reduction of gate resistance by the T-shaped gate with a wide head and improved device performance. This power MHEMT technology can be used toward 77 GHz band applications.

Keywords: 0.15 μm , metamorphic HEMT, T-gate.

I. Introduction

InAlAs/InGaAs high electron mobility transistors (HEMTs) on InP substrates have shown such superiorities as high frequency characteristics, low noise figure, high gain, and efficiency over GaAs-based pseudomorphic HEMTs (PHEMTs) [1], [2]. However, cost, size, and fragility of InP-based HEMTs still remain as obstacles for the commercial uses of InP-based HEMTs to millimeter-wave frequencies.

On the other hand, metamorphic HEMTs (MHEMTs) on a GaAs substrate provide the ability to tailor the lattice constant with wide ranges of indium content, large size, and low cost. Thus, MHEMTs are becoming crucial devices in millimeter-wave monolithic integrated circuits for high power and low-noise applications [3]-[6].

In addition, as a one-chip transceiver consisting of a transmitter and receiver can be readily applicable for system integration, MHEMTs would be especially valuable when the epitaxial structures are adequately engineered so that the transceivers can be fabricated on a wafer. Here, we adopt a power MHEMT with a double-doped structure to realize the transceiver microwave monolithic integrated circuit on a wafer for automotive radar system applications.

Until now, there have been many reports on the power performances of MHEMTs for high power applications [7], [8]. However, there have been few reports on the noise characteristic of a power MHEMT structure.

In this article, we report on the noise performance together with the DC and microwave characteristics, including DC uniformities across 4-inch wafers, of 0.15 μm wide-head T-shape gate GaAs power MHEMTs with an indium content of 53% in an InGaAs channel. The 0.15 μm GaAs power MHEMTs exhibited a very low minimum noise figure of 0.79

Manuscript received Apr. 26, 2005; revised Sept. 9, 2005.

Jae Yeob Shim (phone: + 82 42 860 6212, email: jyshim@etri.re.kr), Hyung-Sup Yoon (email: hsyoon@etri.re.kr), Dong Min Kang (email: kdm1597@etri.re.kr), Ju Yeon Hong (email: jyhong@etri.re.kr), and Kyung Ho Lee (email: khl259@etri.re.kr) are with Basic Research Laboratory, ETRI, Daejeon, Korea.

dB and an associated gain of 10.56 dB at 26 GHz with good DC uniformities.

II. Device Fabrication Process

A schematic of the epitaxial structure of a power MHEMT is shown in Fig. 1. The power MHEMT on a 4-inch semi-insulating GaAs wafer was grown by using a molecular beam epitaxy method. A power MHEMT with double-doped carrier-supplying layers was grown on a graded buffer layer of 120 nm thick InAs/AlAs, followed by a 500 nm thick InAlAs buffer layer. The channel layer was 16 nm thick $\text{In}_{0.53}\text{Ga}_{0.47}\text{As}$. The top and bottom Si-planar doping layers were separated from the channel layer by 3 nm thin $\text{In}_{0.52}\text{Al}_{0.48}\text{As}$ undoped spacer layers, followed by a 16 nm thick $\text{In}_{0.52}\text{Al}_{0.48}\text{As}$ undoped Schottky layer, and a 20 nm thick $\text{In}_{0.53}\text{Ga}_{0.47}\text{As}$ cap layer doped with Si ($5 \times 10^{18} \text{ cm}^{-3}$) for obtaining low ohmic resistance. The room temperature electron mobility of the power MHEMT structure was found to be $9,100 \text{ cm}^2/\text{V}\cdot\text{s}$, and the sheet carrier concentration was $3.5 \times 10^{12} \text{ cm}^{-2}$.

The fabrication procedures of the $0.15 \mu\text{m}$ power MHEMT devices are as follows. After mesa isolation by wet chemical etching using $\text{H}_3\text{PO}_4 : \text{H}_2\text{O}_2 : \text{H}_2\text{O} = 1 : 1 : 50$, ohmic contacts were formed by evaporating AuGe/Ni/Au metallic layers and then alloyed at $340 \text{ }^\circ\text{C}$ using rapid thermal annealing. The obtained ohmic contact resistance is about $1 \times 10^{-6} \Omega\text{cm}^2$. Then, devices with a gate length of $0.15 \mu\text{m}$ and a wide head of $1 \mu\text{m}$ were patterned by electron-beam lithography using PMMA/P(MMA-MAA)/PMMA trilayer resists. To selectively etch the InGaAs ohmic layer over the InAlAs Schottky layer, a gate recess was performed using a mixed solution of succinic acid and H_2O_2 . The etch selectivity of an InGaAs ohmic layer

over an InAlAs Schottky layer higher than 100 was obtained. Then, a Ti/Pt/Au gate metal was deposited using electron-beam evaporator and lifted-off. Finally, to passivate the power MHEMT devices, silicon nitride was deposited by plasma-enhanced chemical vapor deposition. The source-to-drain distance and gate-to-source spacing were $3 \mu\text{m}$ and $1 \mu\text{m}$, respectively. The gate width of the device was $100 \mu\text{m}$.

III. Results and Discussion

A cross-sectional scanning electron microscope (SEM) image of a silicon nitride-passivated wide-head T-shaped gate power MHEMT is shown in Fig. 2. The head width and gate length are about 1.2 and $0.15 \mu\text{m}$, respectively. This T-shaped gate with high aspect ratio (the ratio of gate head width to gate length) is the main reason of the low gate resistance.

The Schottky current-voltage characteristics of the $0.15 \mu\text{m}$ power MHEMT devices were measured at room temperature. The ideality factor of the Schottky diode calculated from the measured forward I-V characteristic was 1.42, and the devices showed good Schottky diode characteristics. A considerably high breakdown voltage of -8.3 V , at which the gate current reaches 1 mA/mm , was also obtained for the power MHEMT devices with a high indium content of 0.53 in the lattice-matched $\text{In}_{0.53}\text{Ga}_{0.47}\text{As}$ channel layer. On the other hand, the measured drain/source breakdown voltages for the device in its 'off-state' and 'on-state' are about 9 and 2.8 V , respectively.

Figure 3 shows the drain currents as a function of source-to-drain voltage for the $0.15 \mu\text{m} \times 100 \mu\text{m}$ power MHEMT devices. The MHEMT devices exhibit complete pinch-off characteristics. The measured drain saturation current is 48 mA at a source-to-drain voltage of 2 V and a source-to-gate voltage

Materials	Layer	Thickness
InGaAs	Cap	20 nm ($5 \times 10^{18} \text{ cm}^{-3}$)
$\text{In}_{0.52}\text{Al}_{0.48}\text{As}$	Schottky	16 nm
Si	Planar doped	$3.5 \times 10^{12} \text{ cm}^{-2}$
$\text{In}_{0.52}\text{Al}_{0.48}\text{As}$	Spacer	3 nm
$\text{In}_{0.53}\text{Ga}_{0.47}\text{As}$	Channel	16 nm
$\text{In}_{0.52}\text{Al}_{0.48}\text{As}$	Spacer	3 nm
Si	Planar doped	$1.5 \times 10^{12} \text{ cm}^{-2}$
$\text{In}_{0.52}\text{Al}_{0.48}\text{As}$	Buffer	500 nm
InAs/AlAs	Graded buffer	120 nm
GaAs	Substrate	

Fig. 1. A schematic of the epitaxial structure of an InGaAs/InAlAs/GaAs MHEMT.

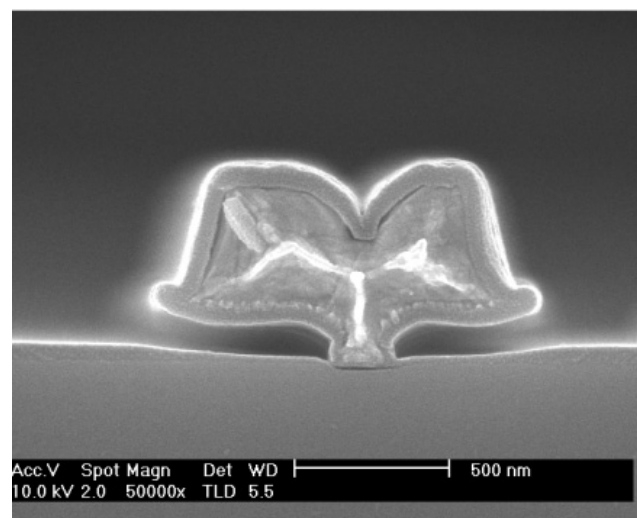


Fig. 2. A cross-sectional SEM image of a SiN-passivated $0.15 \mu\text{m}$ T-gate with wide head.

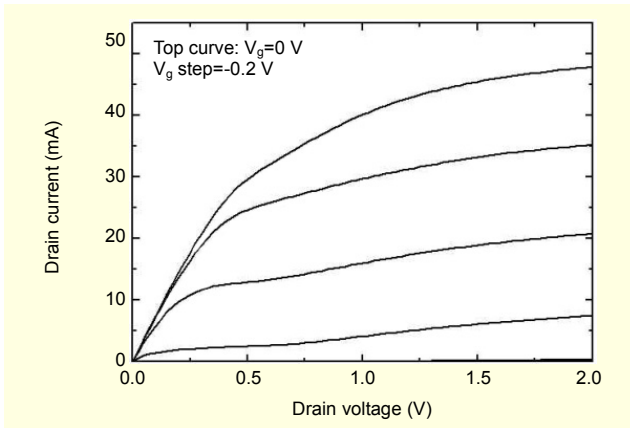


Fig. 3. Current-voltage characteristic for a 0.15 μm MHEMT. The gate-source voltage was changed from 0 to -1.2 V with -0.2 V steps.

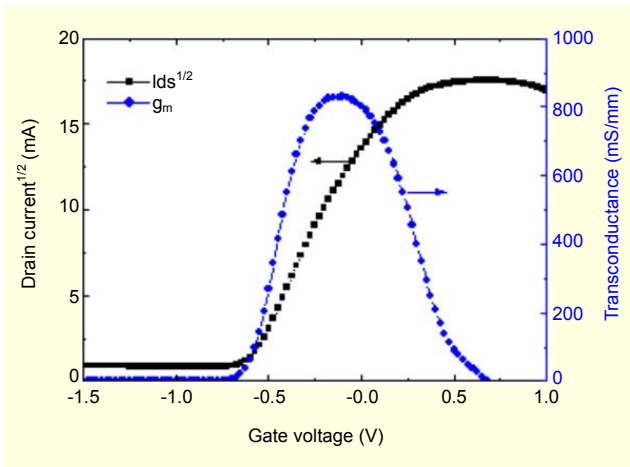


Fig. 4. Drain current and transconductance as a function of gate voltage of a 0.15 μm MHEMT biased at a drain voltage of 1.5 V.

of 0 V.

Figure 4 shows the extrinsic transconductance and drain current (I_{ds}) as a function of gate-to-source voltage (V_{gs}) at a V_{ds} of 1.5 V for the 0.15 $\mu\text{m} \times 100 \mu\text{m}$ power MHEMT devices. The threshold voltage (V_{th}) is defined by a linear extrapolation of the square root of drain current versus gate voltage to zero current. The measured threshold voltage was -0.65 V. The measured maximum extrinsic transconductance is 830 mS/mm at a gate-to-source voltage of -0.13 V.

Highly uniform characteristics of a device are crucial for the fabrication of reproducible integrated circuits. Therefore, we investigated DC uniformities across 4-inch wafers. Figure 5 shows the uniformities of the threshold voltage and maximum extrinsic transconductance characteristics for the 0.15 μm power MHEMT devices across a 4-inch wafer. The average threshold voltage and standard deviation of the threshold voltage were -0.64 V and 30 mV, respectively. The obtained

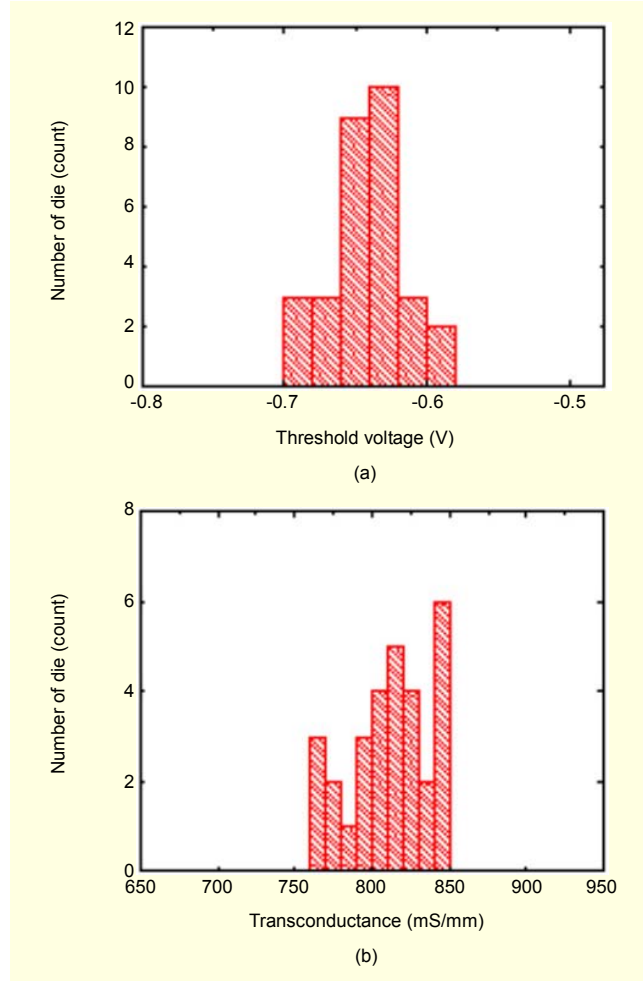


Fig. 5. DC uniformities of the 0.15 μm MHEMT devices across a 4-inch wafer: (a) uniformity of threshold voltage and (b) uniformity of extrinsic transconductance.

uniformity of the threshold voltage was 8.3 %. The average maximum extrinsic transconductance and the standard deviation of the maximum extrinsic transconductance were 810 mS/mm and 25 mS/mm, respectively. The uniformity of the maximum extrinsic transconductance was 5.1%. It is believed that these good uniformities are due mainly to the high etch selectivity of succinic acid.

The s -parameters were measured on a 4-inch wafer using a Cascade microwave probe station and an HP 8510C network analyzer ranging from 1 to 50 GHz. Figure 6 shows the measured current gain ($|h_{21}|$) and MSG/MAG as a function of frequency of a 0.15 $\mu\text{m} \times 100 \mu\text{m}$ power MHEMT device. The cut-off frequency (f_T) was calculated by the extrapolation of $|h_{21}|$ to unity with a -20 dB/decade slope, and the maximum frequency of oscillation (f_{max}) was obtained by the parallel shifting of a -20 dB/decade slope to the MSG/MAG plot. The obtained f_T and f_{max} for the power MHEMT device were 141 and 243 GHz, respectively.

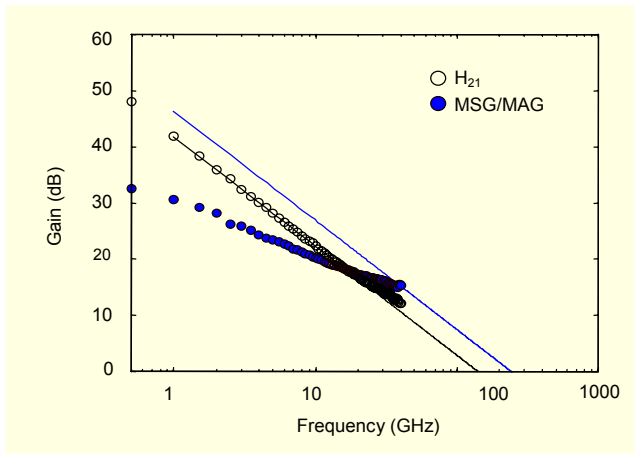


Fig. 6. Frequency dependence of the current gain ($|h_{21}|$) for a $0.15 \mu\text{m}$ MHEMT under a $V_{ds}=1.5 \text{ V}$ and a $V_{gs}=-0.35 \text{ V}$.

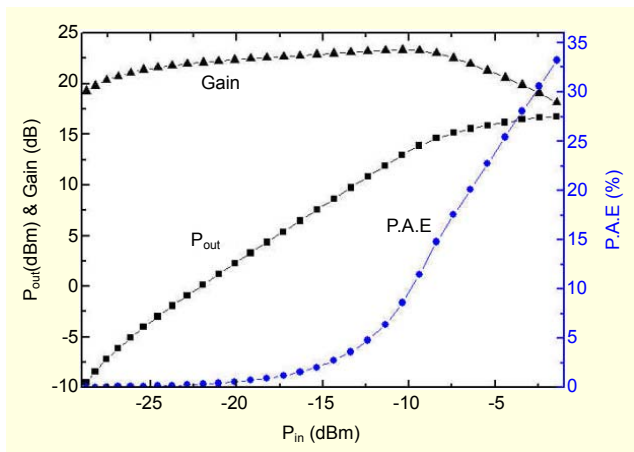


Fig. 7. Measured power output, gain, and PAE of a $8 \times 50 \mu\text{m}$ MHEMT at $V_{ds}=2 \text{ V}$.

These MHEMTs were tested for power performance at 5.8 GHz using a load pull structure with $400 \mu\text{m}$ gate peripheral. The output power, gain, and power-added efficiency (PAE) plots are shown in Fig. 1. The MHEMT device exhibits 33.2% PAE, a 18.1 dB power gain, and 28.17 mW output power.

Finally, noise characteristics of the power MHEMT devices were examined. The noise figure measurements have been carried out in a frequency range between 26 and 40 GHz using an HP 8510C network analyzer, an HP 8970B noise figure meter, and an ATN NP5 noise parameter test set. Figure 8 shows the minimum noise figure (F_{min}) and the associated gain (G_{as}) as a function of frequency at $I_{ds}=7.4 \text{ mA}$ and $V_{ds}=1 \text{ V}$ of the $0.15 \mu\text{m} \times 100 \mu\text{m}$ power MHEMT device. A minimum noise figure of 0.79 dB and an associated gain of 10.56 dB are measured at 26 GHz. At 40 GHz, the measured minimum noise figure and associated gain are 1.21 and 6.41 dB, respectively. Considering the power MHEMT structure with an indium content of 53% in the InGaAs channel, these noise

characteristics are excellent. As shown in Fig. 2, the wide head T-shaped gate exhibited a large cross-sectional area with an aspect ratio of about 8. This high aspect ratio provides a significant reduction of gate resistance. Thus, this low-noise performance can be attributed to the drastic reduction of gate resistance by the T-shaped gate with a wide head [5] and the improved device performance [11].

Previously reported results of an MHEMT are compared with this work in Table 1. Our noise data demonstrated the lowest noise figure minimum among all the others. As these $0.15 \mu\text{m}$ power MHEMT devices show decent noise performances, they can be applicable for the fabrication of the transceivers for millimeter-wave system applications.

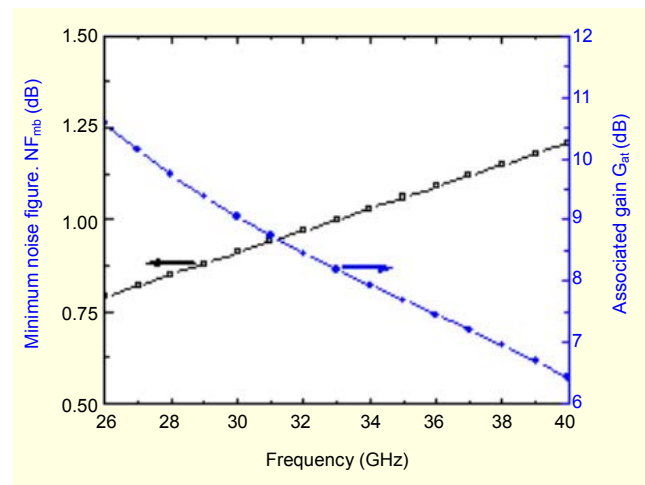


Fig. 8. Minimum noise figure and associated gain as a function of frequency at $V_{ds}=1 \text{ V}$ and $I_{ds}=7.4 \text{ mA}$ of a $0.15 \mu\text{m} \times 100 \mu\text{m}$ power MHEMT.

Table 1. Comparison of the previously published MHEMT data with this work.

Gate length	f_T (GHz)	f_{max} (GHz)	F_{min} (dB@GHz)	Reference
$0.15 \mu\text{m}$	138	-	1.18@25	[4]
$0.1 \mu\text{m}$	120	180	-	[9]
$0.15 \mu\text{m}$	>150	-	0.86@26	[10]
$0.15 \mu\text{m}$	141	243	0.79@26	This work

IV. Conclusions

The noise performances of the $0.15 \mu\text{m}$ gate-length power MHEMTs with double-doped InAlAs/InGaAs structure were investigated together with their DC and microwave characteristics. The $0.15 \mu\text{m} \times 100 \mu\text{m}$ power MHEMT devices showed a high gate-to-drain breakdown voltage of -8.3 V,

an extrinsic transconductance of 830 mS/mm, and a threshold voltage of -0.64 V. In addition, the MHEMT devices exhibited good DC uniformities across a 4-inch GaAs wafer having a V_{th} uniformity of 8.3% and a g_m uniformity of 5.1%. The obtained cut-off frequency and the maximum frequency of oscillation were 141 and 243 GHz, respectively. The $8 \times 50 \mu\text{m}$ MHEMT device shows 33.2% PAE, a 18.1 dB power gain, and 28.2 mW output power. A very low minimum noise figure of 0.79 dB and an associated gain of 10.56 dB were obtained at 26 GHz. Considering the power MHEMT structure with an indium content of 53% in the InGaAs channel, these noise characteristics of the MHEMT devices are excellent. This low-noise performance can be explained by the drastic reduction of the gate resistance by the T-shaped gate with a wide head and improved device performance. These $0.15 \mu\text{m}$ power MHEMT devices can be applicable for the fabrication of transceivers for millimeter-wave system applications.

References

- [1] M.Y. Kao, K.H.G. Duh, P. Ho, and P.C. Chao, "An Extremely Low-Noise InP-Based HEMT with Silicon Nitride Passivation," *IEDM Tech. Dig.*, 1994, p. 907.
- [2] P.M. Smith, S.-M.J. Liu, M.-Y. Kao, P. Ho, S.C. Wang, K.H.G. Duh, S.T. Fu, and P.C. Chao, "W-Band High Efficiency InP-Based Power HEMT with 600 GHz f_{max} ," *IEEE Microwave Guided Wave Lett.*, vol. 5, no. 7, 1995, pp. 230-232.
- [3] M. Zaknour, B. Bonte, C. Gaquiere, Y. Cordier, Y. Druelle, and Y. Crosnier, "InAlAs/InGaAs Metamorphic HEMT with High Current Density and High Breakdown Voltage," *IEEE Electron Device Lett.*, vol. 19, no. 9, 1998, pp. 345-347.
- [4] C.S. Whelan, W.E. Hoke, R.A. MacTaggart, S.M. Lardizabal, P.S. Lyman, P.F. Marsh, and T.E. Kazior, "Low Noise $\text{In}_{0.32}(\text{AlGa})_{0.68}/\text{In}_{0.43}\text{Ga}_{0.57}\text{As}$ Metamorphic HEMT on GaAs Substrate with 850 mW/mm Output Power Density," *Electron Device Lett.*, vol. 21, no. 1, 2000, pp. 5-8.
- [5] J.Y. Shim, H-S. Yoon, S.J. Kim, J.Y. Hong, W.J. Chang, D.M. Kang, J-H. Lee, and K.H. Lee, "DC and Microwave Characteristics of 0.2- μm T-gate Double-Doped Metamorphic InAlAs/InGaAs/GaAs HEMTs Recessed with Succinic Acid/ H_2O_2 ," *J. Korea Phys. Soc.*, vol. 41, no. 4, 2002, pp. 528-532.
- [6] D.M. Kang, J.Y. Hong, J-H. Lee, H-S. Yoon, J.Y. Shim, and K.H. Lee, "A 77GHz MHEMT MMIC Chip Set for Automotive Radar Systems," *ETRI J.*, vol. 27, no. 2, 2005, pp. 133-139.
- [7] M. Kawano, T. Kuzuhara, H. Kawasaki, F. Sasaki, and H. Tokuda, "InAlAs/InGaAs Metamorphic Low-Noise HEMT," *IEEE Microwave Guided Wave Lett.*, vol. 7, no. 1, 1997, pp. 6-8.
- [8] K.C. Hwang, P.C. Chao, C. Creamer, K.B. Nichols, S. Wang, D. Tu, W. Kong, D. Dugas, and G. Patton, "Very High Gain Millimeter-Wave InAlAs/InGaAs/GaAs Metamorphic HEMTs," *IEEE Electron Device Lett.*, vol. 20, no. 11, 1999, pp. 551-553.
- [9] M. Zaknour, M. Ardouin, Y. Cordier, S. Bollaert, B. Bonte, and D. Théron, "60-GHz High Power Performance $\text{In}_{0.35}\text{Al}_{0.65}\text{As}-\text{In}_{0.35}\text{Ga}_{0.65}\text{As}$ Metamorphic HEMTs on GaAs," *Electron Device Lett.*, vol. 24, no. 12, 2003, pp. 724-726.
- [10] M.S. Heins, J.M. Carroll, M. Kao, J. Delaney, and C.F. Campbell, "X-Band GaAs MHEMT LNAs with 0.5 dB Noise Figure," *IEEE MTT-s Symp.*, 2004, p. 149.
- [11] H. Fukui, "Optimal Noise Figure of Microwave GaAs MESFET's," *IEEE Trans. Electron Devices.*, vol. 26, no. 7, 1979, pp. 1032-1037.



Jae Yeob Shim received the BS, MS, and PhD degrees in metallurgical engineering from Yonsei University in Seoul, Korea, in 1991, 1993, and 2000. Since 2000, he has been with Electronics and Telecommunications Research Institute (ETRI), Korea, as a Senior Researcher, where he has been engaged in research on compound semiconductor device fabrication. His research interests are in the developments of GaAs pHEMT, MHEMT, and InP pHEMT devices, especially an e-beam lithography process, and micro-/millimeter wave MMIC for wireless telecommunications systems and their system applications.



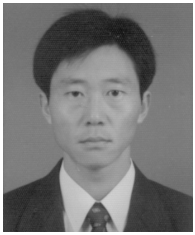
Hyung-Sup Yoon received the BE degree in electronic materials engineering from Kwang Woon University, Korea, in 1980, and the ME and PhD degrees in 1984 and 1991 in applied physics from Inha University, Korea. He joined ETRI in 1984. From 1984 to 1992, he was involved in developing silicon processes and devices. Since 1993, he has been a Principal Researcher in the High Speed IC Research Department in ETRI. His current research interests include the process development, fabrication, and characterization of low-noise GaAs and InP-based HEMT devices for millimeter wave MMIC applications.



Dong Min Kang received the MS degree in electronics engineering from Kwangwoon University, Seoul, Korea. From 1998 to 2000, he was with MCC, where he worked on RF module developments for wireless telecommunications. In 2000, he joined ETRI, where he has been engaged in research on micro-/millimeter wave MMIC design for wireless telecommunications systems and automotive collision avoidance systems. Since 2004, he has been a member of Senior Research Staff of the High Speed IC Research Department of ETRI. His research interests include MMIC design, RF front-end module development, and packaging.



Ju Yeon Hong received the MS degree in electronics engineering from Dongguk University, Seoul, Korea. In 2001, she joined ETRI, where she has been engaged in research on micro-/millimeter wave MMIC design for wireless telecommunications systems and automotive collision avoidance systems. Since 2004, she has been a member of Research Staff of the High Speed IC Research Department of ETRI. Her research interests include MMIC design and packaging.



Kyung Ho Lee received the BS and MS degrees in metallurgical engineering from Seoul National University in Seoul, Korea, in 1980 and 1982. He earned the PhD degree in materials science and engineering from Stanford University in Stanford, USA, in 1989. From 1989 to 1996, he was with ETRI of Korea as a member of Senior Research Staff, where he has been engaged in R&D on advanced compound semiconductor device fabrication. From 1996 to 1998, he was with Eaton Semiconductor Korea, where he was the Director of Applications, heading the troubleshooting and development of Eaton ion implanter-related processes and hardware. In 1998, he rejoined ETRI as a member of Principal Research Staff of Compound Semiconductor Department to manage national research projects on micro-/millimeter-wave MMIC developments for wireless telecommunications and THz optical communications systems. He also headed in establishing the basis of a foundry service of ETRI's 4" compound semiconductor fabrication facility. He is currently leading up the InP IC team. His research interests are in the development of advanced compound semiconductor devices and ICs for their system applications.